Title

Domoic acid disrupts the activity and connectivity of neuronal networks in organotypic brain slice cultures

Authors

Hiolski, EM
Ito, S
Beggs, JM
et al.

Publication Date

2016-09-01

DOI

10.1016/j.neuro.2016.08.004

Peer reviewed

HHS Public Access

Author manuscript

Neurotoxicology. Author manuscript; available in PMC 2017 September 01.

Published in final edited form as:

Neurotoxicology. 2016 September ; 56: 215–224. doi:10.1016/j.neuro.2016.08.004.

Domoic acid disrupts the activity and connectivity of neuronal networks in organotypic brain slice cultures

EM Hiolski[#a], **S Ito**[#b], **JM Beggs**[c], **KA Lefebvre**[d], **AM Litke**[b], and **DR Smith**[a]

[a]Department of Microbiology & Environmental Toxicology, University of California, Santa Cruz, CA, USA

[b]Santa Cruz Institute for Particle Physics, University of California, Santa Cruz, CA, USA

[c]Department of Physics, Indiana University, Bloomington, IN, USA

[d]Northwest Fisheries Science Center, NOAA Fisheries, Seattle, WA, USA

[#] These authors contributed equally to this work.

Abstract

Domoic acid is a neurotoxin produced by algae and is found in seafood during harmful algal blooms. As a glutamate agonist, domoic acid inappropriately stimulates excitatory activity in neurons.At high doses, this leads to seizures and brain lesions, but it is unclear how lower, asymptomatic exposures disrupt neuronal activity. Domoic acid has been detected in an increasing variety of species across a greater geographical range than ever before, making it critical to understand the potential health impacts of low-level exposure on vulnerable marine mammal and human populations. To determine whether prolonged domoic acid exposure altered neuronal activity in hippocampal networks, we used a custom-made 512 multi-electrode array with high spatial and temporal resolution to record extracellular potentials (spikes) in mouse organotypic brain slice cultures. We identified individual neurons based on spike waveform and location, and measured the activity and functional connectivity within the neuronal networks of brain slice cultures. Domoic acid exposure significantly altered neuronal spiking activity patterns, and increased functional connectivity within exposed cultures, in the absence of overt cellular or neuronal toxicity. While the overall spiking activity of neurons in domoic acid-exposed cultures was comparable to controls, exposed neurons spiked significantly more often in bursts. We also identified a subset of neurons that were electrophysiologically silenced in exposed cultures, and putatively identified those neurons as fast-spiking inhibitory neurons. These results provide evidence that domoic acid affects neuronal activity in the absence of cytotoxicity, and suggest that neurodevelopmental exposure to domoic acid may alter neurological function in the absence of clinical symptoms.

Correspondence to: AM Litke; DR Smith.

Keywords

domoic acid; multielectrode recording; developmental neurotoxicity; organotypic brain slice culture

1. Introduction

Domoic acid is a neurotoxin produced by algae and is found in seafood during harmful algal blooms. It can harm marine wildlife and humans by causing excitotoxicity in the central nervous system through over-stimulation of glutamate receptors (AMPA and kainate receptors) (Perl et al., 1990; Scholin et al., 2000; Stewart et al., 1990). Acute domoic acid exposure at high doses is well-known to cause seizures and neuronal death (Teitelbaum et al., 1990; Tryphonas et al., 1990), but the neurological impacts of lower-dose, sub-clinical exposure are not well-known. As domoic acid is becoming increasingly prevalent in the marine environment due to increases in harmful algal bloom frequency over an expanding geographical range (Anderson et al., 2012; Hallegraeff, 1993; Lefebvre et al., 2016; Moore et al., 2008), marine wildlife and humans are at heightened risk for domoic acid exposure. Recently, an unprecedented domoic acid-producing harmful algal bloom caused by a large warm-water anomaly persisted through all of summer 2015 along the Pacific coast of North America (NOAA, 2015). This bloom severely poisoned hundreds of sea lions and led to the closing of several important fisheries in California, Oregon, and Washington. California sea lions regularly ingest domoic acid at concentrations reaching mg/kg levels during harmful algal blooms (Bejarano et al., 2007). Multiple marine species will likely face increasing exposure risk in the future as ocean temperatures continue to rise.

The developing fetus of pregnant mammals may be at particular risk because domoic acid crosses the placenta, is retained in amniotic fluid, and enters the fetal brain (Maucher & Ramsdell, 2007), and neonatal domoic acid exposure can also occur through breast milk (Maucher & Ramsdell, 2005, 2007). This is especially concerning because domoic acid's disruption to the developing glutamate system, even at exposures below those that cause seizures, can produce neurological effects lasting into adulthood (Costa et al., 2010). For example, neonatal rats exposed to sub-clinical doses of domoic acid daily over postnatal days 8-14 exhibit a number of neurological and hippocampal alterations as adults. These include increased axon sprouting, increased neurotrophic factor/receptor expression (Bernard et al., 2007; Doucette et al., 2004), reduction in a GABAergic subpopulation of neurons (Gill et al., 2010), novelty-induced seizures (Doucette et al., 2004), modified stress response, increased perseveration, and altered search strategy (Gill et al., 2012). While these studies provide clear evidence of cellular/molecular and behavioral responses to developmental domoic acid exposure, there is little information about how neuronal activity and functional connectivity is affected, or how changes in hippocampal circuit development may contribute to these reported functional deficits.

Electrophysiological studies of neuronal activity can help bridge the findings of sub-clinical domoic acid exposure's cellular/molecular and behavioral impacts. For example, recording the activity of hundreds of neurons from within the same brain region can give insight into

the functional networks these neurons form, how they communicate with one another, and observe what changes arise from treatment with domoic acid. In contrast, recordings of individual neurons' activity can answer questions about a compound's affects on the function and physiology of an individual cell, but these findings are difficult to extrapolate into effects on circuits of neurons that mediate regional function. Similarly, larger-scale imaging of activity in the functioning brain (e.g., functional MRI) lacks the resolution to reflect cellular details, leaving a gap in our ability to understand what happens in a population of individual neurons. Gaining a better understanding of how domoic acid influences the electrophysiological activity and connectivity of neural networks could provide insight into how cellular effects translate into behavioral outcomes.

We investigated the effect of sub-cytotoxic domoic acid exposure on the electrophysiological activity and connectivity of neural networks in organotypic hippocampal slice cultures, using a custom-made 512 multi-electrode array that provided very fine spatial and temporal resolution (Litke et al., 2004). We hypothesized that domoic acid exposure, in the absence of overt cytotoxicity, would increase the activity and connectivity of neuronal networks due to elevated glutamatergic activity. Specifically, we quantified both neuron-level activity outcomes – including spike rate and burst rate – and network-level parameters (e.g., connectivity density) to address the knowledge gap between known domoic acid-induced cellular/molecular changes and changes in whole-brain function and behavior.

2. Methods

2.1 Organotypic brain slice cultures & domoic acid exposure

Cortico-hippocampal organotypic cultures (n=37) were prepared from seven mouse pups (age postnatal day 6; five-six slice cultures per brain) following the methods described by Stoppini et al. (1991). Briefly, brains were extracted, blocked into a cube (~5 mm per side) containing the hippocampus, and sectioned at 400 μm with a vibrating blade microtome (Leica VT1000 S). The sections were trimmed to include only the hippocampus and overlying cortex, and placed on circular filter paper (hydrophile membrane PTFE ~6 mm diameter, 0.4 μm pore size; BioCell Interface, Switzerland). Cultures were grown in culture media (1 mL per culture: 50% minimum essential medium (MEM), 25% horse serum, 25% Hank's balanced salt solution, 5 mg/mL D-glucose, 1 m*M* L-glutamine, and 5 U/mL penicillin-streptomycin) and maintained in an incubator for 16-17 days at 37°C and 5% CO_2 (see Ito et al. (2014) for more details). All animal care and treatments were approved by the institutional IACUC and adhered to NIH guidelines set forth in the Guide for the Care and Use of Laboratory Animals (NRC, 2011).

Half-volume (500 μL) culture media changes were done every 3 days, beginning the day after culture preparation (day 1 *in vitro*, DIV1). Cultures were pseudo-randomly assigned to control (n=18) and domoic acid (n=19) treatment groups; assignments were balanced across cultures that originated from the same mouse. Exposure to 0.1 μ*M* domoic acid began on DIV4, using culture media containing domoic acid, and continued through DIV16-17.

This domoic acid dose was selected to be below those shown to cause overt cytotoxicity in organotypic cultures: our dose is 10–15-fold lower than the ≥1 to 5 μ*M* levels shown to

cause reduced cell viability in the CA1, CA3 and dentate gyrus in hippocampal brain slice cultures (A Pérez-Gómez & Tasker, 2012). Domoic acid concentrations in culture media aliquots collected prior to and following organotypic culture exposures were determined by ELISA (Biosense Laboratories, Bergen, Norway) and found to be 0.12 ± 0.019 μM (mean ± SD, n=18), which was not measurably different from the expected 0.1 μM target dose.

2.2 Multi-electrode array recording & spike-sorting

Electrophysiological activity from brain slice cultures (n=14 control, n=15 domoic acid) was recorded on DIV16 or 17 using a custom-made 512-electrode array system (Litke et al., 2004). This array features flat electrodes 5 μm in diameter and spaced 60 μm apart in a hexagonal lattice over a 0.9 mm × 1.9 mm rectangular area. Cultured brain tissues and adherent filter paper were gently placed on the electrode array, tissue-side down, with the hippocampal region centered on the array. A small, circular weight (~1.3 g) with fine mesh (160 mm pore size) was placed on the filter paper on top of the tissue to maintain even contact between the tissue and the array. The recording chamber (~1.8 mL volume) housing the array and mounted tissue was filled with fresh culture media (no domoic acid), and was kept perfused with culture medium (95% O_2, 5% CO_2, 37°C) at a flow rate of 3 mL/min.

Prior to electrophysiological recording, tissues were equilibrated in the recording chamber for 30 min to avoid any transient activity that could have been caused by temperature differences from moving the culture from the incubator to the chamber. Extracellular signals from neuronal action potentials (spikes) were recorded for 90 minutes on each of the 512 electrode channels at a sampling rate of 20 kHz (i.e., 50 μsec temporal resolution). Raw waveforms were then spike-sorted using methods developed by Litke et al. (2004). Briefly, spike-sorting uses the electrophysiological activity recorded by each electrode to identify individual neurons based on the timing, waveform, and location of spiking activity on the array (see Supplemental Information for more details). This method significantly extends the information gained by simply assessing electrophysiological activity at each electrode, because more than one neuron may be contributing to the activity detected by a single electrode. Our spike-sorting analyses allowed us to evaluate individual neurons' electrophysiological activity.

2.3 Identification of hippocampal neurons in electrophysiological recordings

In general, the hippocampi of mouse organotypic brain slice cultures were slightly smaller than the array, covering ~70-80% of the recording area (Fig S1). Because some activity from cortical neurons was occasionally included at the margins of the array, we identified and selected hippocampal neurons for analysis. This was accomplished using a photographic overlay process, in which we compared brightfield photomicrographs of the cultures taken on DIV1, which exhibits the clearest visual tissue morphology, and again after recording on DIV 16 or 17, including the 512-array. The map of identified neurons from each recording, determined through spike-sorting analyses (section 2.2), were plotted on top of the corresponding tissue's DIV1 photograph to visualize with the underlying anatomical structures. Only electrophysiologically active neurons within the hippocampal region were retained for further analysis of the hippocampal network structure (see Ito et al. (2014) for additional detail).

2.4 Neuronal spike rate and bursting activity assessment

Spike rate was defined as the number of spikes (action potentials) a neuron produces per second across the 90-minute electrophysiological recording, while burst rate was defined as the number of bursts a neuron produces per minute over the 90-minute recording. To calculate how often hippocampal neurons spiked in bursts, we used a modified Poisson surprise algorithm (Stafford et al., 2009). This method uses the mean inter-spike interval (the average time between each action potential) of a neuron to define the criteria that a particular neuron needs to meet for its spikes to qualify as a burst. When the inter-spike interval for a series of 3+ spikes was less than half the mean inter-spike interval, and the probability that such an event occurred by chance was less than 10^{-4}, then that cluster of spikes was defined as a burst. Thus, burst rate (bursts/min) measured the degree to which a neuron spiked exclusively in temporally concentrated clusters of spikes. That is, a neuron with a high burst rate spiked in distinct temporal bands, with inactivity in between each burst; a neuron with a low burst rate spiked at regular intervals, at any spike rate, and did not have distinct, alternating periods of activity/inactivity (see Supplemental Information for more details).

2.5 Effective connectivity density measurement by transfer entropy analysis

Connectivity density was defined as the percentage of connected neuron pairs out of the total number of possible neuron pairs on the array. We used transfer entropy to calculate the functional connectivity density – as opposed to physical connections – within the neural networks of recorded tissues. Physical connections, such as synapses between neurons, are not always electrophysiologically active (i.e., “silent” synapses), and not all neurons exhibit spontaneous electrophysiological activity in organotypic brain slice cultures; effective connectivity instead describes information flow and correlated activity patterns between active neurons. Transfer entropy is an information-theoretic calculation that identifies interactions between two neurons based on the timing of their spikes (action potentials) (Ito et al., 2011). In this calculation, a neuron pair is identified as connected when the spike history of neuron 1 improves the ability to predict the spiking activity of neuron 2 beyond the prediction based on neuron 2’s spike history alone. That is, when two neurons spike in a temporally synchronous pattern, the transfer entropy calculation will be more positive than a neuron pair that does not spike synchronously (Shimono & Beggs, 2014).

Equations and algorithm details/parameters can be found in the Supplemental Information. Also see Ito et al. (2011), Shimono & Beggs (2014) & Timme et al. (2014) for more discussion of transfer entropy and its applications in analyzing the neural networks of organotypic brain slice cultures.

2.6 Immunohistochemistry & imaging

Immediately after electrophysiological recording, photographs of all organotypic cultures on the 512-electrode array were taken using a Nikon CoolPix 995 camera mounted on a Leica DM IL inverted microscope to record the exact location of the tissue on the microelectrode array. Immediately following imaging, the cultures were gently lifted from the array and fixed in 4% paraformaldehyde for 20 minutes, then stored in phosphate buffered saline with 0.05% sodium azide at 4°C. The eight non-recorded cultures were also fixed/stored in the same manner on DIV17.

For NeuN immunostaining of neurons, brain slice cultures (n=10 control: 6 recorded, 4 non-recorded; n=12 domoic acid: 8 recorded, 4 non-recorded) were processed free-floating. Antibodies used were: mouse monoclonal IgG1 anti-NeuN (neuronal nuclei – Chemicon Millipore (cat #MAB377), 1:1000); goat anti-mouse IgG (Molecular Probes Alexa Fluor 555, 1:1000). A 10-min DAPI incubation (Invitrogen D21490/DAPI-Fluoro- Pure Grade, 300 n*M* working solution) was included to stain for cell nuclei. Cultures were mounted, coverslipped with Fluoromount-G (Southern Biotech), and allowed to dry overnight before imaging. (See Supplement for full protocol.)

For staining-based cell counts, cultures were imaged on a Keyence Biorevo BZ-9000 digital widefield microscope using a 40×/0.95 objective lens; exposure time was optimized to the z-plane of highest-intensity staining for each field of view in each culture. All other microscope and imaging parameters were kept constant. One z-stack (0.6 μm spacing) per channel (both DAPI and NeuN) was captured within each hippocampal sub-region (CA1, CA3, and DG) per culture.

2.7 Cell counts

Cell counts were performed on the z-stack images taken at 40× magnification using ImageJ/FIJI (NIH) and the Surfaces algorithm of Imaris software (BitPlane, Concord, MA). We used both voxel intensity and size thresholds for NeuN (intensity threshold = 10; size thresholds = ≥5 μm, ≥2000 voxels) and DAPI (intensity threshold = 35; size thresholds = ≥7 μm, ≥2000 voxels) labeling. The number of surfaces detected by the algorithm yielded the number of total cells ($DAPI^+$) and neurons ($NeuN^+$).

2.8 Statistics

All data are given as means ± standard error of the mean (SE) or least squares mean ± standard error, as indicated. For cell and neuron counts (both immunostained and electrophysiologically active) and connectivity density, a mixed model ANOVA was used to assess differences between control and domoic acid-exposed cultures, with treatment as a fixed effect and the animal each culture originated from a random effect. For neuron-level outcomes (spike rate & burst rate), the random effect was modified so that the organotypic culture that each neuron was measured in was nested within the animal that the culture was generated from. For the percent bursting and percent putative inhibitory neuron outcomes, a binomial regression was used to assess the differences in cell-type proportions within control and domoic acid-exposed cultures. Data for NeuN count, spike rate, and burst rate were log-transformed, and connectivity density was logit transformed to achieve Gaussian distribution prior to analyses. JMP Pro 12.0.1 (SAS Institute Inc., Cary, NC, USA) was used for statistical analyses. Statistical significance is indicated as follows: $*p < 0.05$, $**p < 0.01$, $***p < 0.005$.

3. Results & Discussion

3.1 Domoic acid exposure was not overtly cytotoxic

We used a domoic acid exposure level (0.1 μ*M*) that was <10% of levels (i.e., 1 - 5 μ*M*) that have been shown to cause reduced cell viability in brain slice cultures (A Pérez-Gómez &

Tasker, 2012). To confirm that our low-dose domoic acid exposure paradigm did not cause overt cell or neuronal toxicity, we conducted total cell and neuron counts in the hippocampi of organotypic brain slice cultures using DAPI and NeuN immunohistochemical staining. Results show that domoic acid exposure had no measurable effect on either total cell numbers or the number of neurons (total cells, $DAPI^+$ in the CA1, $F(1,15.8) = 0.12$, $p = 0.74$; CA3, $F(1,13.2) = 0.65$, $p = 0.43$; and dentate gyrus (DG), $F(1,16.7) = 0.50$, $p = 0.49$), (neurons, $NeuN^+$ cells in the CA1, $F(1,14.9) = 0.08$, $p = 0.79$; CA3, $F(1,14.6) = 2.07$, $p = 0.17$; and DG, $F(1,12.0) = 0.08$, $p = 0.78$) (Fig. 1D and 1E). The proportion of neurons to total cells within was also not affected (Fig. S3).

3.2 Domoic acid exposure reduced the number of electrophysiologically active neurons

In order to determine whether the number of electrophysiologically active neurons in the hippocampus was affected by domoic acid exposure, we identified all active neurons by spike-sorting the action potentials recorded by the 512-array (see Methods) and specifically selected neurons within the hippocampus (Fig. 2A). We found that domoic acid-exposed brain slice cultures had significantly fewer active hippocampal neurons than control cultures (Fig. 2B, Table S1) (control 134 ± 21.9 neurons, least squares mean ± SE), domoic acid 93.8 ± 21.6 neurons; $F(1,22.5) = 6.76$, $p = 0.016$). Taken with the previous finding that the total number of neurons was not affected (Fig. 1), this suggests that a subset of neurons were electrophysiologically silenced following prolonged *in vitro* low level domoic acid exposure. Note that although the number of active hippocampal neurons should be a subset of the number of hippocampal neurons in the brain slice culture measured by immunostaining, those two datasets cannot be directly compared because the fields of view for microscopy analyses do not specifically correspond to the area measured by the 512-electrode array.

This reduction in the number of active neurons may be attributed to the presence of “silent” synapses in the domoic acid-exposed cultures. Physical synapses may be functionally silent and non-responsive to synaptic transmission through removal of AMPA receptors from the synaptic membrane (Isaac et al., 1995; Liao et al., 1995). AMPA receptors are a specific sub-type of glutamate receptor that domoic acid binds to with strong affinity (i.e., 9 n*M*) (Carcache et al., 2003; Hampson & Manalo, 1998; Hampson et al., 1992). Persistent, weak synaptic stimulation – perhaps similar to that caused by prolonged low dose domoic acid exposure – has been shown to cause a weakening of functional synaptic connections due to internalization of AMPA receptors from the neuron membrane (Czöndör & Thoumine, 2013; Hanse et al., 2013). AMPA receptor internalization is mediated through dephosphorylation of the receptor, and interestingly, domoic acid exposure (400 n*M* for 1 hour) has been shown to decrease AMPA receptor phosphorylation in rat hippocampal slice cultures (Qiu et al., 2009). While our data do not directly prove or identify a specific mechanism for neuron silencing, it is plausible that neurons responded to prolonged domoic acid exposure by altering their activity or excitability to compensate for the excitatory environment in which they were cultured. After removal from the domoic acid-contaminated media 30 min prior to recording, any persistent compensatory changes in the neuronal activity would be measured by the 512-array during recording.

3.3 Domoic acid exposure did not significantly alter neuronal spike rate, but significantly increased neuronal bursting activity

In order to broadly assess how domoic acid exposure altered electrophysiological activity patterns in the neural networks of brain slice cultures, we visually examined neural activity profiles and raster plots. Neuron activity profiles (Fig. 3A, B) show the average spiking rate of all hippocampal neurons over the 90-minute duration of the recording. For example, in brain slice culture ID 3-1 (Fig. 3A), 104 hippocampal neurons were identified through spike-sorting (see Methods), and the spike rates of all neurons within a 1-second time period were averaged for each of the 5400 seconds (90 min) of electrophysiological recording (x-axis). The representative activity profiles shown provide qualitative evidence of alterations caused by domoic acid exposure – for example, a lower baseline activity (red arrows, right y-axis) and greater number of large-amplitude spike rates (arrowheads, top of figure panels) (Fig. 3A, B; see Fig. S4 for all activity profiles). Raster plots of representative 1 min segments of neuronal activity illustrate individual neurons' spikes over time (Fig. 3C, D). Qualitative visual assessment of the raster plots revealed that there were generally fewer fast-spiking neurons in the domoic acid-exposed brain slice cultures compared to controls (arrows in Fig. 3C, D; Fig. S5). These differences suggest that domoic acid exposure altered activity patterns in the neural networks of organotypic brain slice cultures.

In order to quantify these observed changes in electrophysiological activity, we calculated both the spike rate (spikes/sec in Hz) and burst rate (bursts/min) of hippocampal neurons in all control and domoic acid-exposed brain slice cultures. Spike rate was calculated on a per-neuron basis by dividing each neuron's total number of recorded spikes by the recording duration (5400 sec). Burst rate (i.e., the number of bursts a neuron produced per minute) was calculated with a modified Poisson surprise algorithm (see Methods).

We found no difference in the mean spike rate (Hz) of active neurons in domoic acid-exposed cultures compared to neurons in control cultures (control 0.32 ± 0.02 Hz (least squares mean ± SE), domoic acid 0.29 ± 0.02 Hz; $F(1,24.6) = 1.46$, $p = 0.24$) (Fig. 4, Table S1). However, there was a significant increase in the proportion of bursting vs non-bursting neurons in domoic acid-exposed vs control cultures (control 91.6 ± 3.1%, domoic acid 96.8 ± 1.2%; $p = 0.0041$) (Fig. 5A, Table S1). The burst rate of bursting neurons was also significantly increased in domoic acid-exposed cultures compared to neurons in control cultures (control 0.43 ± 0.04 min^{-1} (least squares mean ± SE), domoic acid 0.67 ± 0.07 min^{-1}; $F(1,24.5) = 8.80$, $p = 0.0066$) (Fig. 5B, Table S1).

In other studies, short-term domoic acid exposure (~10 minutes at 0.5 - 2 μ*M*; ~30 - 60 minutes at ~3 - 1000 μ*M*) reduced the mean spike rate (spikes/sec) in primary mixed neuronal/glial cortical cell cultures in a dose-dependent manner (Hogberg et al., 2011; Mack et al., 2014; Wallace et al., 2015). Mean burst rate (bursts/min, where a burst is defined as ≥5 spikes in 100 msec) was also reduced by short-term/acute exposure to domoic acid (~10 minutes at 0.5 - 2 μ*M*) (Hogberg et al., 2011). Interestingly, in the same mixed cell culture model, prolonged exposure (28 - 35 days *in vitro*) to 50 n*M* domoic acid actually *increased* the mean spike rate and mean burst rate (Hogberg et al., 2011). Notably, domoic acid was present in the culture medium during all of these recordings, suggesting that the reported

increases in spike and burst rate were due to the excitatory effect of domoic acid on neuron activity during electrophysiological recording.

In our study, brain slice cultures were washed with domoic acid-free medium for 30 minutes prior to recording, and subsequently recorded in domoic acid-free medium. This allowed us to measure the effects of prolonged domoic acid exposure on neuronal activity in brain slice cultures that underwent growth/development in an excitatory environment. Our findings that domoic acid exposure increased neuronal burst rate (bursts/min) without affecting mean spike rate (Hz) suggests that domoic acid exposure altered the *pattern* of neuronal activity, but not the overall activity as reflected by the mean spike rate. In the absence of changes in total neuronal network activity, it is possible that altered activity patterns may affect how neurons interact with one another within the network.

3.4 Domoic acid increased the functional connectivity density in electrophysiologically active neurons

In order to quantify changes in functional connectivity within the neural networks of organotypic brain slice cultures, we calculated the 'connectivity density' within each culture. Connectivity density is defined as the percentage of hippocampal neuron pairs identified as electrophysiologically connected out of all possible active neuron pairs. Here, connectivity density measures functional connectivity, as opposed to physical connectivity; that is, it provides information on the electrophysiological activity within the neural network, rather than a count of physical synapses (Ito et al., 2011).

We found that domoic acid exposure increased connectivity density from 1.39% (± 0.24%) in control cultures to 2.73% (± 0.50%) in domoic acid-exposed cultures ($F(1,22.7) = 8.61$, $p = 0.0075$) (Fig. 6). This increase in functional connectivity is consistent with changes in physical connectivity that have been shown with domoic acid exposure in previous studies. For example, increased mossy fiber sprouting, a form of abnormal synaptic reorganization within the dentate gyrus of the hippocampus, has been documented in domoic acid-exposed brain slice cultures (Anabel Pérez-Gómez & Tasker, 2013), domoic acid-exposed sea lions (Buckmaster et al., 2014), and lab rats exposed to domoic acid in the early pre-weaning lifestage (Bernard et al., 2007). Enhanced synapse formation, as measured by the pre- and post-synaptic markers synaptophysin and PSD-95, respectively, has also been reported in brain slice cultures in response to domoic acid exposure (2 μ*M* for 24 hours) (Anabel Pérez-Gómez & Tasker, 2013).

3.5 Domoic acid exposure caused the silencing or loss of a subset of fast-spiking neurons

In order to quantify the silencing/loss of fast-spiking neurons in the domoic acid-exposed brain slice cultures (red arrows on right y-axis, Fig. 3C versus 3D, section 3.3), we explored whether these neurons exhibited a distinct electrophysiological activity phenotype based on their spike rate (Hz) and burst rate (bursts/min). As these neurons appeared to be continuously spiking at regular intervals (i.e., high spike rate with low burst rate), we set a "high spike rate" criteria of ≥5 Hz and a "low burst rate" criteria of ≤1 burst/min (see insets in Fig. 7A, B). Plotting individual neurons' spike rate versus burst rate (Fig. 7A, B) in control and domoic acid-exposed cultures showed that the proportion of fast-spiking neurons

(proportion of total active neurons) was significantly reduced in domoic acid-exposed brain slice cultures compared to controls (control 4.16% ± 0.68% of total neurons, domoic acid 0.87% ± 0.23%; $p = 0.0002$) (Fig. 7C, Table S1).

To further characterize the phenotype of this subset of neurons, we examined the nature of their functional connections with other neurons. For this, we produced cross-correlation histogram plots for each set of functional neuron pairs to reflect the condensed spike-timing relationship between the connected neuron pairs (Ito et al., 2014). We qualitatively assessed the cross-correlation histograms for the 86 fast-spiking neurons (74 control, 12 domoic acid) identified in control and domoic acid-exposed cultures to determine whether there was clear evidence of an active connection (i.e., inhibitory trough or excitatory peak to the right of zero; see Fig. 7D for an example of a cross-correlation histogram). Of the 86 identified fast-spiking neurons, 64 neurons showed clear evidence of active connections: in control cultures 53 fast-spiking neurons showed evidence of 75 total active connections, and in domoic acid-exposed cultures 11 fast-spiking neurons showed evidence of 19 active connections. Of these 64 neurons, we found that 35 neurons exhibited inhibitory connections (28 control, 7 domoic acid), 2 neurons exhibited excitatory connections (1 control, 1 domoic acid), while the remainder (27 neurons) did not exhibit a pattern of connectivity that was sufficiently clear to categorize as inhibitory or excitatory (i.e., lacked a trough or peak). Thus, of the 37 neurons that we were able to confidently categorize in the control and domoic acid-exposed cultures, 95% exhibited inhibitory connections with other neurons. Based on this, we putatively identified the fast-spiking neurons as inhibitory neurons. Our conclusion that these ‘putative inhibitory’ (PI) neurons were largely silenced/lost in the domoic acid-exposed cultures is consistent with evidence that domoic acid exposure reduces inhibitory activity (as measured by inhibitory post-synaptic potentials) in brain slice cultures following exposure to high-affinity kainite receptor agonists, including domoic acid (1 μ*M*) (Clarke & Collingridge, 2004).

One intriguing possibility is that these silenced/lost PI neurons are fast-spiking/parvalbumin$^+$ interneurons. Fast-spiking/parvalbumin$^+$ neurons are a subset of GABAergic neurons that spike very rapidly and help regulate excitatory activity in the hippocampus, and they play important roles in basic microcircuit functions and complex network operations (Hu et al., 2014). Fast-spiking/parvalbumin$^+$ interneurons comprise ~2.6% of hippocampal neurons (Hu et al., 2014) and ~5% of cortical neurons (Behrens & Sejnowski, 2009), which corresponds closely to the proportion of PI neurons (4.2%) that we measured in control cultures. Although we cannot determine here the mechanism through which these PI neurons were silenced/lost with domoic acid treatment, one possibility is that, as GABAergic neurons are known to express AMPA receptors (Y. He et al., 1998; Racca et al., 1996), they internalized AMPA receptors as a compensatory response to prolonged stimulation by domoic acid treatment. Inhibitory neurons normally maintain a high proportion of silent synapses, regardless of developmental period/window (Hanse et al., 2013), and are highly sensitive to changes in glutamatergic activity (S. He & Bausch, 2014). Also, the slow development of parvalbumin$^+$ neurons may increase their vulnerability to domoic acid exposure during neurodevelopment, and permanently affect their maturation and function (Behrens & Sejnowski, 2009). Domoic acid-induced disruptions to the activity of this

critical sub-population of neurons, even in the absence of seizures and cell death, would likely have impacts on normal brain function lasting into adulthood.

Conclusions

Prolonged sub-clinical domoic acid exposure altered the activity pattern and connectivity density of neural networks in organotypic brain slice cultures, and silenced a subset of fast-spiking neurons that we putatively identified as inhibitory neurons. These kinds of electrophysiological alterations have been linked to neurological dysfunction *in vivo*, which underscores the potential for neurodevelopmental domoic acid exposure to cause lasting effects on neurological function. This is especially critical for domoic acid-exposed wildlife, as disruption to spatial learning and memory could reduce foraging and survival success. The custom-made 512 multielectrode array technology and computational data analysis tools used here provided the ability to investigate neural network activity and function with single-neuron specificity. This level of detailed electrophysiological study will help fill important knowledge gaps that bridge findings of the effects of sub-clinical domoic acid exposure on cellular/molecular processes with behavioral impacts.

Supplementary Material

Refer to Web version on PubMed Central for supplementary material.

Acknowledgements

The authors would like to thank Preston Kendrick (NOAA Fisheries) for ELISA measurements of domoic acid, Ben Abrams (UCSC Microscopy Center) for assistance with microscopy and quantification software, Fang-Chin Yeh for training on organotypic slice culture preparation, and Daniel Kirsner (UCSC Applied Math and Statistics Dept) for statistics advice and guidance. Funding sources: NSF IIS-0904413 (to SI & AML); NSF DGE-0809125-006 (to EMH); (NIH) R01 ES021930 (to KAL and David Marcinek, University of Washington); (NSF) OCE-1314088 (to KAL and David Marcinek, University of Washington); UCSC COR (to EMH & DRS); Friends of Long Marine Lab (to EMH & DRS); Meyers Oceanographic Trust (to EMH & DRS).

References

Anderson DM, Cembella AD, Hallegraeff GM. Progress in Understanding Harmful Algal Blooms: Paradigm Shifts and New Technologies for Research, Monitoring, and Management. Annual Review of Marine Science. 2012; 4(1):143–176.

Behrens MM, Sejnowski TJ. Does schizophrenia arise from oxidative dysregulation of parvalbumin-interneurons in the developing cortex? Neuropharmacology. 2009; 57(3):193–200. [PubMed: 19523965]

Bejarano AC, Van Dolah FM, Gulland FM, Schwacke L. Exposure assessment of the biotoxin domoic acid in California sea lions: Application of a bioenergetic model. Marine Ecology Progress Series. 2007; 345:293–304.

Bernard PB, Macdonald DS, Gill DA, Ryan CL, Tasker RA. Hippocampal Mossy Fiber Sprouting and Elevated trkB Receptor Expression Following Systemic Administration of Low Dose Domoic Acid During Neonatal Development. Hippocampus. 2007; 17:1121–1133. [PubMed: 17636548]

Buckmaster PS, Wen X, Toyoda I, Gulland FMD, Van Bonn W. Hippocampal neuropathology of domoic acid-induced epilepsy in California sea lions (Zalophus californianus). The Journal of comparative neurology. 2014; 522(7):1691–706. [PubMed: 24638960]

Carcache LM, Rodriguez J, Rein KS. The structural basis for kainoid selectivity at AMPA receptors revealed by low-mode docking calculations. Bioorganic & medicinal chemistry. 2003; 11(4):551–9. Retrieved from http://www.ncbi.nlm.nih.gov/pubmed/12538020. [PubMed: 12538020]

Clarke VRJ, Collingridge GL. Characterisation of the effects of ATPA, a GLU(K5) kainate receptor agonist, on GABAergic synaptic transmission in the CA1 region of rat hippocampal slices. Neuropharmacology. 2004; 47(3):363–72. [PubMed: 15275825]

Costa LG, Giordano G, Faustman EM. Domoic acid as a developmental neurotoxin. Neurotoxicology. 2010; 31(5):409–23. [PubMed: 20471419]

Czöndör K, Thoumine O. Biophysical mechanisms regulating AMPA receptor accumulation at synapses. Brain Research Bulletin. 2013; 93:57–68. [PubMed: 23174308]

Doucette TA, Bernard PB, Husum H, Perry MA, Ryan CL, Tasker RA. Low doses of domoic acid during postnatal development produce permanent changes in rat behaviour and hippocampal morphology. Neurotoxicity research. 2004; 6(7-8):555–63. Retrieved from http://www.ncbi.nlm.nih.gov/pubmed/15639787. [PubMed: 15639787]

Gill DA, Perry MA, McGuire EP, Pérez-Gómez A, Tasker RA. Low-dose neonatal domoic acid causes persistent changes in behavioural and molecular indicators of stress response in rats. Behavioural brain research. 2012; 230(2):409–17. [PubMed: 22387806]

Gill DA, Ramsay SL, Tasker RA. Selective reductions in subpopulations of GABAergic neurons in a developmental rat model of epilepsy. Brain research. 2010; 1331:114–23. [PubMed: 20331981]

Hallegraeff GM. A review of harmful algal blooms and their apparent global increase. Phycologia. 1993; 32(2):79–99.

Hampson DR, Huang XP, Wells JW, Walter JA, Wright JL. Interaction of domoic acid and several derivatives with kainic acid and AMPA binding sites in rat brain. European journal of pharmacology. 1992; 218(1):1–8. Retrieved from http://www.ncbi.nlm.nih.gov/pubmed/1383007. [PubMed: 1383007]

Hampson DR, Manalo JL. The activation of glutamate receptors by kainic acid and domoic acid. Natural toxins. 1998; 6(3-4):153–8. Retrieved from http://www.ncbi.nlm.nih.gov/pubmed/10223631. [PubMed: 10223631]

Hanse E, Seth H, Riebe I. AMPA-silent synapses in brain development and pathology. Nature reviews. Neuroscience. 2013; 14(12):839–50. [PubMed: 24201185]

He S, Bausch SB. Synaptic plasticity in glutamatergic and GABAergic neurotransmission following chronic memantine treatment in an in vitro model of limbic epileptogenesis. Neuropharmacology. 2014; 77:379–86. [PubMed: 24184417]

He Y, Janssen WG, Vissavajjhala P, Morrison JH. Synaptic distribution of GluR2 in hippocampal GABAergic interneurons and pyramidal cells: a double-label immunogold analysis. Experimental neurology. 1998; 150(1):1–13. [PubMed: 9514819]

Hogberg HT, Sobanski T, Novellino A, Whelan M, Weiss DG, Bal-Price AK. Application of micro-electrode arrays (MEAs) as an emerging technology for developmental neurotoxicity: Evaluation of domoic acid-induced effects in primary cultures of rat cortical neurons. NeuroToxicology. 2011; 32(1):158–168. [PubMed: 21056592]

Hu H, Gan J, Jonas P. Interneurons. Fast-spiking, parvalbumin^{+} GABAergic interneurons: from cellular design to microcircuit function. Science (New York, N.Y.). 2014; 345(6196):1255263.

Isaac JTR, Nicoll RA, Malenka RC. Evidence for silent synapses: Implications for the expression of LTP. Neuron. 1995; 15(2):427–434. [PubMed: 7646894]

Ito S, Hansen ME, Heiland R, Lumsdaine A, Litke AM, Beggs JM. Extending transfer entropy improves identification of effective connectivity in a spiking cortical network model. PloS one. 2011; 6(11):e27431. [PubMed: 22102894]

Ito S, Yeh F-C, Hiolski E, Rydygier P, Gunning DE, Hottowy P, Timme N, Litke AM, Beggs JM. Large-scale, high-resolution multielectrode-array recording depicts functional network differences of cortical and hippocampal cultures. PloS one. 2014; 9(8):e105324. [PubMed: 25126851]

Lefebvre KA, Quakenbush L, Frame E, Huntington KB, Sheffield G, Stimmelmayr R, Bryan A, Kendrick P, Ziel H, Goldstein T, Snyder JA, Gelatt T, Gulland F, Dickerson B, Gill V. Prevalence of algal toxins in Alaskan marine mammals foraging in a changing arctic and subarctic environment. Harmful Algae. 2016; 55:13–24. [PubMed: 28073526]

Liao D, Hessler N. a, Malinow R. Activation of postsynaptically silent synapses during pairing-induced LTP in CA1 region of hippocampal slice. Nature. 1995

Litke AM, Bezayiff N, Chichilnisky EJ, Cunningham W, Dabrowski W, Grillo AA, Grivich M, Grybos P, Hottowy P, Kachiguine S, Kalmar RS, Mathieson K, Petrusca D, Rahman M, Sher A. What Does the Eye Tell the Brain?: Development of a System for the Large-Scale Recording of Retinal Output Activity. IEEE Transactions on Nuclear Science. 2004; 51(4):1434–1440.

Mack CM, Lin BJ, Turner JD, Johnstone AFM, Burgoon LD, Shafer TJ. Burst and principal components analyses of MEA data for 16 chemicals describe at least three effects classes. Neurotoxicology. 2014; 40:75–85. [PubMed: 24325902]

Maucher JM, Ramsdell JS. Domoic Acid Transfer to Milk: Evaluation of a Potential Route of Neonatal Exposure. Environmental Health Perspectives. 2005; 113(4):461–464. [PubMed: 15811837]

Maucher JM, Ramsdell JS. Maternal-fetal transfer of domoic acid in rats at two gestational time points. Environmental health perspectives. 2007; 115(12):1743–6. [PubMed: 18087593]

Moore SK, Trainer VL, Mantua NJ, Parker MS, Laws EA, Backer LC, Fleming LE. Impacts of climate variability and future climate change on harmful algal blooms and human health. Environmental Health. 2008; 7(Suppl 2):S4.

NOAA. Record-setting bloom of toxic algae in North Pacific. 2015. Climate.gov

NRC. Guide for the Care and Use of Laboratory Animals. 8th ed.. The National Academies Press; Washington D.C.: 2011.

Pérez-Gómez A, Tasker RA. Enhanced neurogenesis in organotypic cultures of rat hippocampus after transient subfield-selective excitotoxic insult induced by domoic acid. Neuroscience. 2012; 208:97–108. [PubMed: 22366222]

Pérez-Gómez A, Tasker RA. Enhanced Mossy Fiber Sprouting and Synapse Formation in Organotypic Hippocampal Cultures Following Transient Domoic Acid Excitotoxicity. Neurotoxicity research. 2013; 25(4):402–10. [PubMed: 24347374]

Perl TM, Bedard L, Kosatsky T, Hogkin JC, Todd ECD, Remis RS. An outbreak of toxic encephalopathy caused by eating mussels contaminated with domoic acid. New England Journal of Medicine. 1990; 322:1775–80. [PubMed: 1971709]

Qiu S, Jebelli AK, Ashe JH, Currás-Collazo MC. Domoic acid induces a long-lasting enhancement of CA1 field responses and impairs tetanus-induced long-term potentiation in rat hippocampal slices. Toxicological sciences : an official journal of the Society of Toxicology. 2009; 111(1):140–50. [PubMed: 19564213]

Racca C, Catania MV, Monyer H, Sakmann B. Expression of AMPA-glutamate receptor B subunit in rat hippocampal GABAergic neurons. The European journal of neuroscience. 1996; 8(8):1580–1590. [PubMed: 8921250]

Scholin CA, Gulland F, Doucette GJ, Benson S, Busman M, Chavez FP, Cordaro J, DeLong R, De Vogelaere A, Harvey J, Haulena M, Lefebvre K, Lipscomb T, Loscutoff S, Lowenstine LJ, Marin R, Miller PE, Van Dolah FM. Mortality of sea lions along the central California coast linked to a toxic diatom bloom. Nature. 2000; 403(6765):80–4. [PubMed: 10638756]

Shimono M, Beggs JM. Functional Clusters, Hubs, and Communities in the Cortical Microconnectome. Cerebral Cortex. 2014:1–15.

Stafford BK, Sher A, Litke AM, Feldheim DA. Spatial-temporal patterns of retinal waves underlying activity-dependent refinement of retinofugal projections. Neuron. 2009; 64(2):200–12. [PubMed: 19874788]

Stewart GR, Zorumski CF, Price MT, Olney JW. Domoic acid: a dementia-inducing excitotoxic food poison with kainic acid receptor specificity. Experimental neurology. 1990; 110(1):127–38. Retrieved from http://www.ncbi.nlm.nih.gov/pubmed/2170163. [PubMed: 2170163]

Stoppini L, Buchs P. a, Muller D. A simple method for organotypic cultures of nervous tissue. Journal of neuroscience methods. 1991; 37(2):173–82. Retrieved from http://www.ncbi.nlm.nih.gov/pubmed/1715499. [PubMed: 1715499]

Teitelbaum JS, Zatorre RJ, Carpenter S, Gendron D, Evans AC, Gjedde A, Cashman NR. Neurologic sequelae of domoic acid intoxication due to the ingestion of contaminated mussels. New England Journal of Medicine. 1990; 322(25):1781–7. [PubMed: 1971710]

Timme N, Ito S, Myroshnychenko M, Yeh F-C, Hiolski E, Hottowy P, Beggs JM. Multiplex Networks of Cortical and Hippocampal Neurons Revealed at Different Timescales. PLoS ONE. 2014; 9(12):e115764. [PubMed: 25536059]

Tryphonas L, Truelove J, Nera E, Iverson F. Acute neurotoxicity of domoic acid in the rat. Toxicologic pathology. 1990; 18(1 Pt 1):1–9. [PubMed: 2362984]

Wallace K, Strickland JD, Valdivia P, Mundy WR, Shafer TJ. A multiplexed assay for determination of neurotoxicant effects on spontaneous network activity and viability from microelectrode arrays. NeuroToxicology. 2015; 49:79–85. [PubMed: 26027956]

HIGHLIGHTS

- Domoic acid is a neurotoxin produced by algae during harmful algal blooms.
- Domoic acid altered the activity pattern and connectivity density of neural networks.
- Domoic acid silenced a subset of putatively identified inhibitory fast-spiking neurons.
- Findings suggest domoic acid exposure may alter neurological function without clinical symptoms.

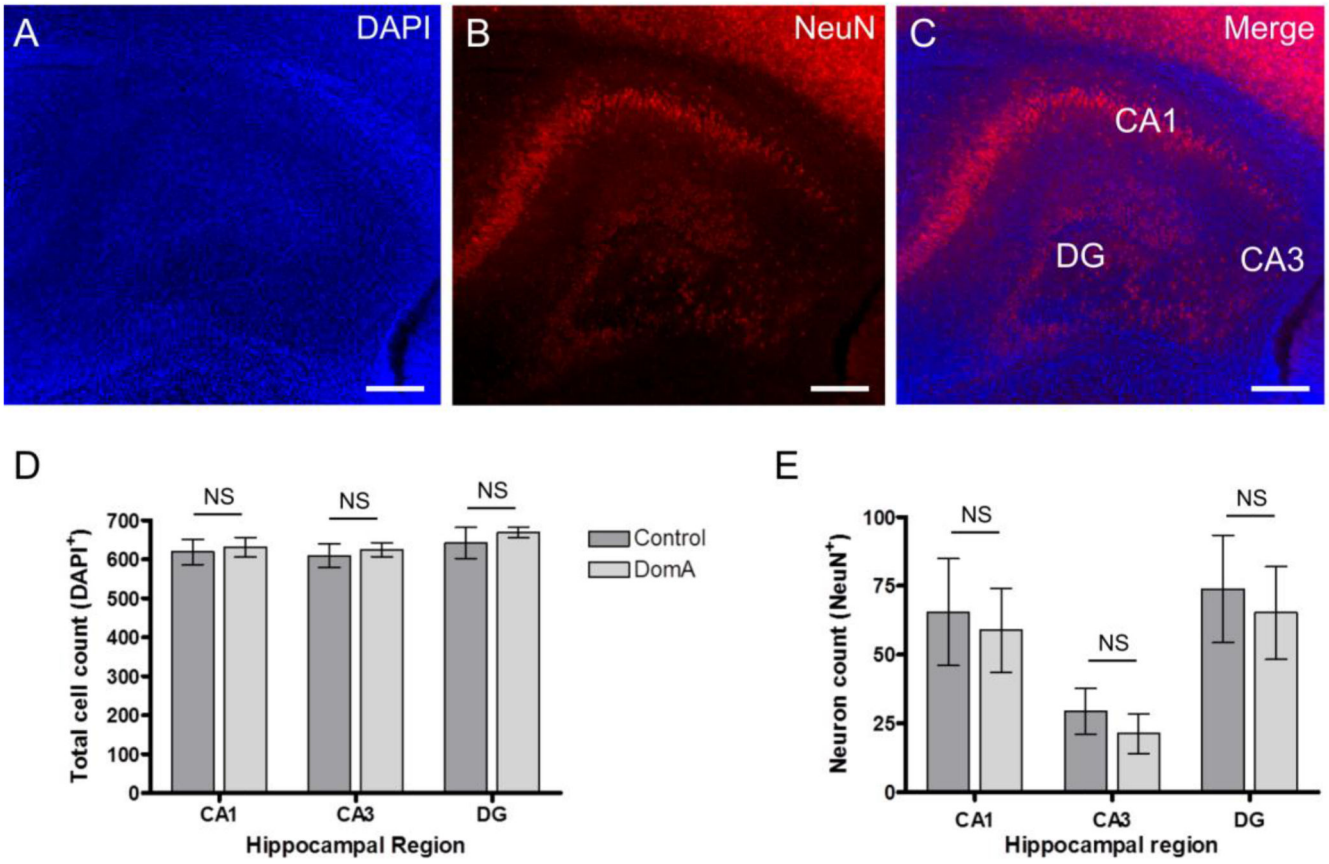

Figure 1. The number of total cells or neurons was not affected by domoic acid exposure

Immunostaining and quantification of neurons ($NeuN^+$) and total cells ($DAPI^+$) in the hippocampi of organotypic brain slice cultures. (A-C) Representative organotypic brain slice culture (brain slice ID 6-6; ×4 magnification) stained with DAPI (A) (blue; labels all cell nuclei) and NeuN (B) (red; labels neuronal nuclei), and merge (C), with hippocampal subregions CA1, CA3, dentate gyrus (DG) indicated. Scale bar = 200 μm. Quantification of total cell (D) and neuron (E) counts per hippocampal subregion for both control (n=10, mean ± SE) and domoic acid-exposed (n=12) tissue cultures. NS = not significantly different, $p > 0.05$ for all (mixed model ANOVA).

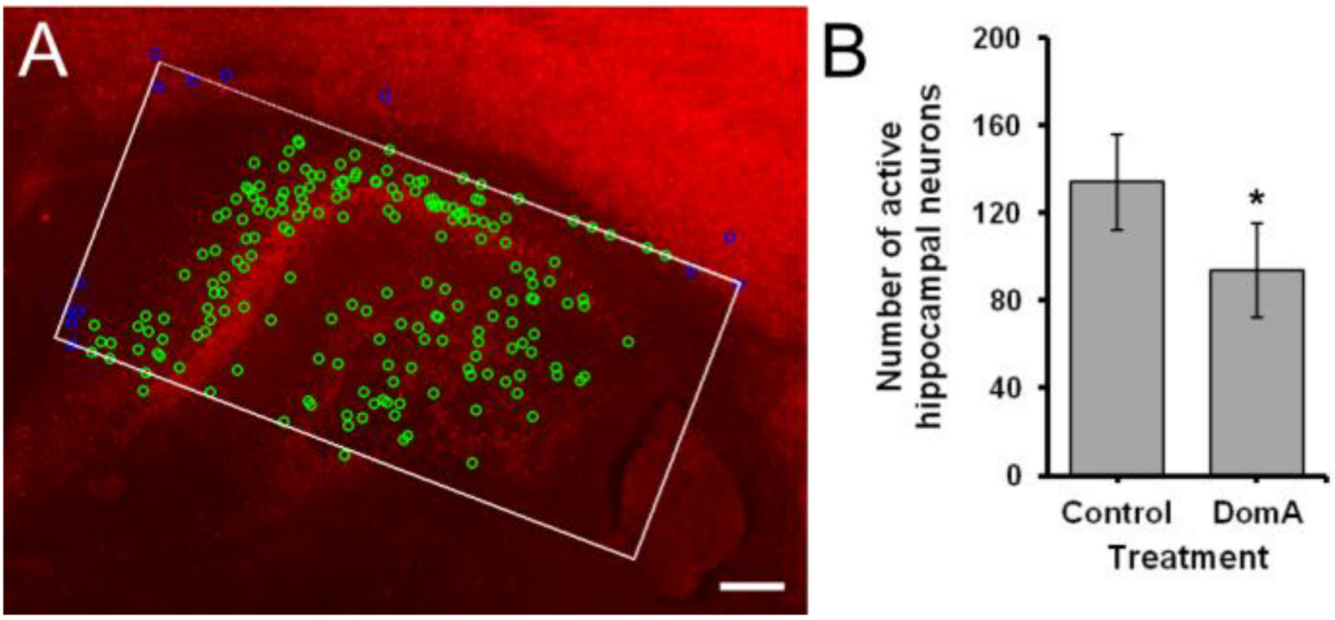

Figure 2. The number of electrophysiologically active neurons in the hippocampi of brain slice cultures was reduced by domoic acid exposure

(A) Photomicrograph (×4 magnification; scale bar = 200 μm) of a representative brain slice culture (red staining = $NeuN^+$ neurons). White box highlights the region covered by the 512-electrode array, and electrophysiologically identified neurons (circles) are overlaid. Green circles = hippocampal neurons; blue circles = cortical neurons (excluded from analyses). (B) Number of electrophysiologically active hippocampal neurons (least squares mean ± SE) in control (n=14) and domoic acid-exposed (n=15) brain slice cultures. * $p < 0.05$ (mixed model ANOVA).

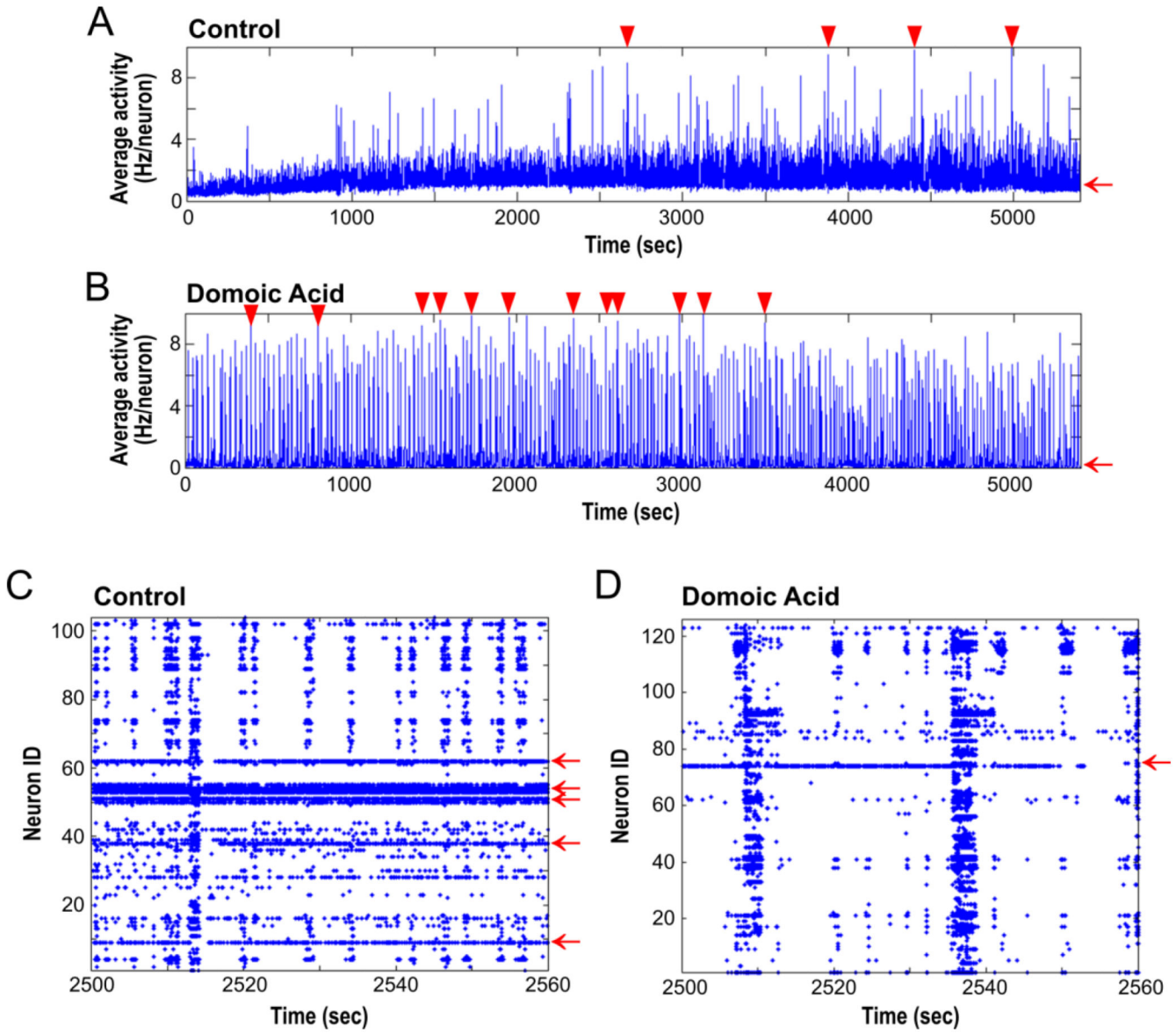

Figure 3. The pattern of electrophysiological activity in brain slice cultures was altered by domoic acid exposure

Electrophysiological activity profiles for representative control and domoic acid-exposed brain slice cultures. (A & B) Activity traces show average electrophysiological activity (Hz/neuron) of representative (A) control (tissue ID 3-1; 104 active neurons), and (B) domoic acid-exposed (tissue ID 3-2; 126 active neurons) brain slice cultures over the 90 minute duration of the recording. (C & D) Raster plots for a representative 60 sec interval of the recordings shown in A & B illustrate spike activity for each individual neuron. Neuron ID is shown along the y-axis, and individual dots (·) indicate one action potential (spike) for each neuron. Note the decrease in the number of fast-spiking neurons (red arrows, right y-axis) between the control (C) and domoic acid-exposed (D) tissues.

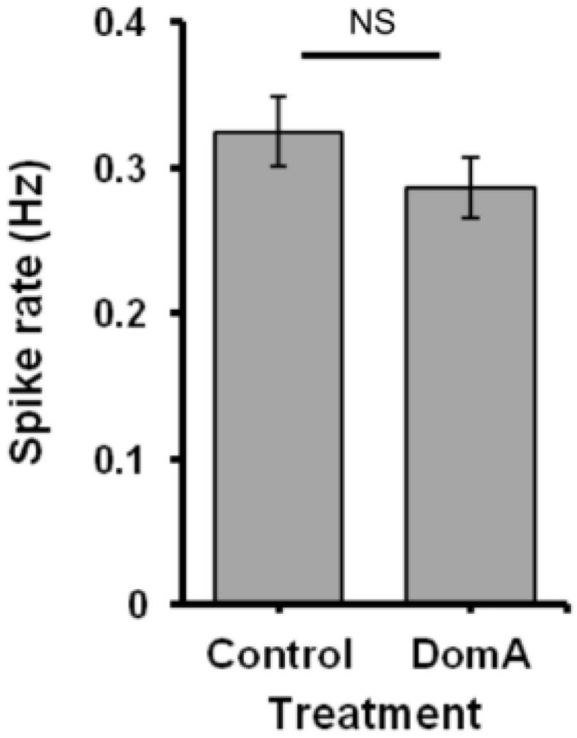

Figure 4. Spike rate (Hz) of active neurons in brain slice cultures was not affected by domoic acid exposure

Spike rate of hippocampal neurons in control (n=14 cultures; n=23 - 264 neurons per culture) and domoic acid-exposed (n=15 cultures; n=22 - 206 neurons per culture) brain slice cultures. NS = not significantly different (p=0.24, mixed model ANOVA).

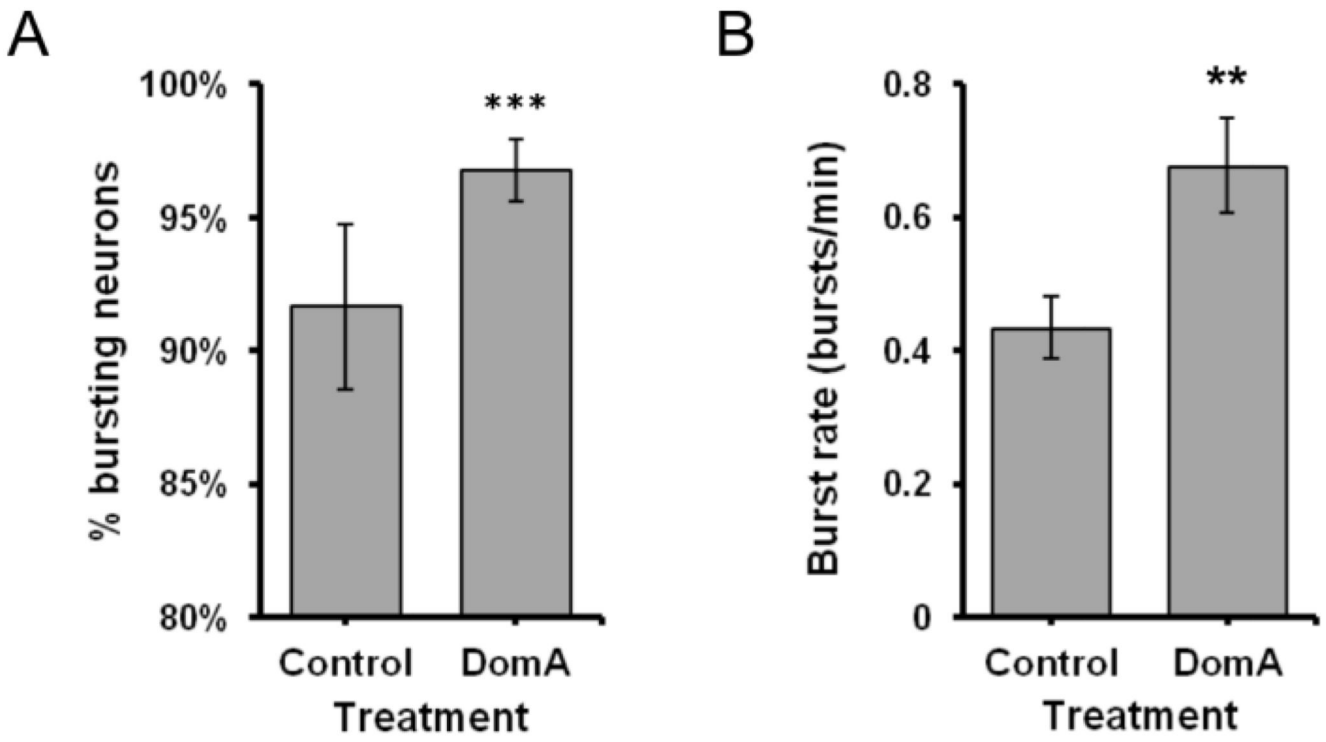

Figure 5. The burst rate (bursts/min) of active neurons was increased by domoic acid exposure

(A) Percentage of hippocampal neurons exhibiting bursting activity (mean ± SE) within control (n=14) and domoic acid-exposed (n=15) cultures (*** $p < 0.005$, binomial regression). (B) Neuron burst rate (bursts/min; mean ± SE per culture) of hippocampal neurons in control (n=14 cultures; n=14 - 254 neurons per culture) and domoic acid-exposed (n=15 cultures; n=20 - 203 neurons per culture) brain slice cultures (** $p < 0.01$, mixed model ANOVA).

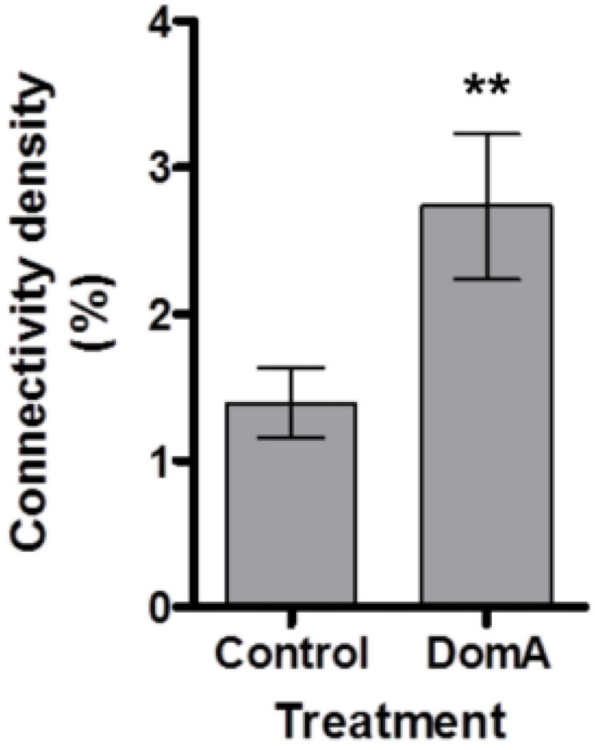

Figure 6. Connectivity density within the neural networks of brain slice cultures was increased by domoic acid exposure

Connectivity density (mean ± SE) within the hippocampal networks of control (n=14) and domoic acid-exposed (n=15) brain slice cultures. Connectivity density is the percentage of all possible active neuron pairs that are functionally connected as determined by their coordinated spiking activity (**$p < 0.01$, mixed model ANOVA).

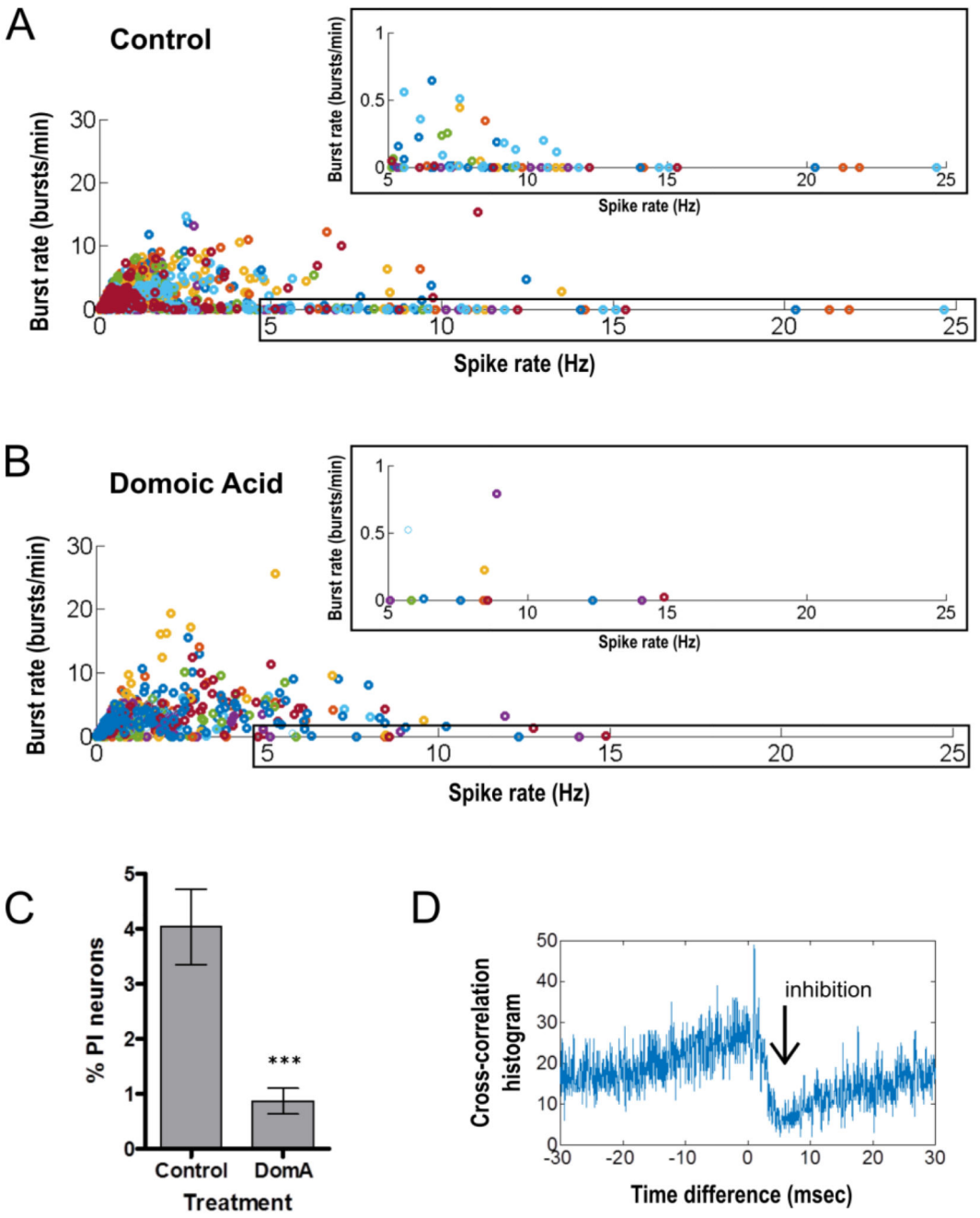

Figure 7. Identification, quantification, and characterization of putative inhibitory neurons silenced in domoic acid-exposed brain slice cultures

(A, B) Constantly spiking neurons, characterized by a high spike rate (Hz) and low burst rate (bursts/min), are shown in the boxed area of the x-axis and expanded in the inset panels; the number of these constantly spiking neurons are reduced in domoic acid-exposed (B) versus control (A) brain slice cultures. All neurons from all recorded cultures are included; symbol color corresponds to individual cultures (n=14 control, n=15 domoic acid). (C) Quantification of the percentage of these putatively inhibitory (PI) neurons within control and domoic acid-exposed cultures (***$p < 0.0005$, binomial regression). (D) Cross-

correlation histogram for a representative PI neuron; cross-correlation histograms illustrate the relationship of one neuron's spiking activity with another's. For example, if neuron A has an excitatory effect on neuron B, whenever neuron A spikes, neuron B will spike immediately afterward, and there will be a peak in the cross-correlation histogram between 0 and 10 msec. Alternatively, if neuron A has an inhibitory effect on neuron B, there will be a trough between 0 and 10 msec. In panel D, the depression between 0 and 10 msec (arrow) indicates that neuron A (PI neuron) suppressed the spiking activity in the second neuron.